

Division - Soil Processes and Properties | Commission - Soil Chemistry

Aggregate Stability in Soil with Humic and Histic Horizons in a Toposequence under Araucaria Forest

Daniel Hanke^{(1)*} and Deborah Pinheiro Dick⁽²⁾

⁽¹⁾ Universidade Federal do Pampa, *Campus Dom Pedrito*, Dom Pedrito, Rio Grande do Sul, Brasil.

⁽²⁾ Universidade Federal do Rio Grande do Sul, Instituto de Química, Porto Alegre, Rio Grande do Sul, Brasil.

ABSTRACT: Aggregate stability is one of the most important factors in soil conservation and maintenance of soil environmental functions. The objective of this study was to investigate the aggregate stability mechanisms related to chemical composition of organic matter in soil profiles with humic and histic horizons in a toposequence under Araucaria moist forest in southern Brazil. The soils sampled were classified as Humic Hapludox (highest position), Fluvaquentic Humaquepts (lowest slope position), and Typic Haplosaprists (floodplain). The C and N contents were determined in bulk soil samples. The chemical composition of soil organic matter was evaluated by infrared spectroscopy. Aggregate stability was determined by applying increasing levels of ultrasound energy. Carbon content increased from the top of the slope to the alluvial plain. Higher ultrasonic energy values for clay dispersion were observed in the C-rich soils in the lower landscape positions, indicating that organic compounds play an important role in the structural stabilization of these profiles. Both aliphatic and carbohydrate-like structures were pertinent to aggregate stability. In the Oxisol, organo-mineral interaction between carbohydrates and the clay mineral surface was the most important mechanism affecting aggregation. In soils with a higher C content (Humaquepts and Haplosaprists), stabilization is predominantly conferred by the aliphatic groups, which is probably due to the structural protection offered by these hydrophobic organic groups.

Keywords: carbon, soil structure, ultrasound energy, organo-mineral interaction, hydrophobicity.

* Corresponding author:

E-mail: hankesolos@gmail.com

Received: September 1st, 2016

Approved: January 2, 2017

How to cite: Hanke D, Dick DP. Aggregate stability in soil with humic and histic horizons in a toposequence under Araucaria forest. Rev Bras Cienc Solo. 2017;41:e0160369.

<https://doi.org/10.1590/18069657rbcsc20160369>

Copyright: This is an open-access article distributed under the terms of the Creative Commons Attribution License, which permits unrestricted use, distribution, and reproduction in any medium, provided that the original author and source are credited.



INTRODUCTION

Soil aggregate stability is one of the most important factors for soil conservation and maintenance of soil environmental functions. Aggregation affects soil capacity to store and stabilize organic C (Six et al., 2004; Kodešová et al., 2008), as well as soil water storage capacity and distribution in the landscape (Scheer et al., 2011; Schmidt et al., 2011; Berhe and Kleber, 2013). In addition, an increase in soil structural stability increases resistance against erosive agents and compaction (Schmidt et al., 2011; Novara et al., 2012; Berhe and Kleber, 2013; Chaplot and Cooper, 2015).

Aggregate stability is defined by several intrinsic soil properties. In soil profiles with lower soil organic matter (SOM) content, the main aggregation agents are Fe and Al oxides. The effect of these minerals on aggregate stability has been attributed to structural cementation, and is a subject extensively explored in the literature (Goldberg et al., 1988; Seta and Karathanasis, 1996; Pinheiro-Dick and Schwertmann, 1996; Barthès et al., 2008; Igwe et al., 2009). However, in soils with lower clay and Fe oxide content, aggregate stability is related to SOM (Six et al., 2002).

The relation between C content and aggregate stability was observed in soils in tropical climates in different degrees of weathering (Chaney and Swift, 1984; Gajic et al., 2006; Six et al., 2004; Inda Junior et al., 2007; Li et al., 2007). The SOM effect on aggregation has traditionally been attributed to the inner sphere complexes between the carboxyl groups and cations of the mineral structure by the ligand exchange mechanism (Chorover and Amistadi, 2001; Mikutta et al., 2011). Other types of organo-mineral interactions are also proposed: i) hydrophobic interactions; ii) C-O-alkyl groups and mineral hydroxyls; iii) cation bridges; iv) anion and cation exchange; and v) Van der Waals interactions (Stumm, 1992; Dick et al., 2009; Hanke et al., 2015). However, the effects of these organo-mineral interactions on aggregate stability have not been investigated in detail.

In mineral soils, the positive effect of SOM on aggregation is usually related to its content (Six et al., 2002; Wiseman and Püttmann, 2005; Inda Junior et al., 2007; Kodešová et al., 2009). However, the role of SOM chemical composition on aggregate stability has been less investigated.

Soil organic matter is composed of hydrophilic structures, such as carboxyl, N, and C-O-alkyl groups, as well as hydrophobic structures, such as aliphatic and aromatic groups. Recent theoretical models hold that hydrophilic groups, which are abundant in oxidizing environments, interact directly with the mineral surface; this occurs mainly with Fe and Al oxides, due to their high density of monocoordinated hydroxyls (Krull et al., 2003; Schöning et al., 2005; Wiseman and Püttmann, 2006; Mikutta et al., 2011). Some studies have indicated that in aerobic soils, the surface of Fe oxides can interact directly with carbohydrate-like structures that are more labile compounds, and not only via ligand exchange with carboxyl groups (Miltner and Zech, 1998; Schöning et al., 2005).

The SOM zonal model (Wershaw et al., 1996; Kleber et al., 2007) proposes that organo-mineral interactions occur between the mineral surface and the organic hydrophilic groups, while the aliphatic and aromatic structures constitute sites for hydrophobic interaction with other SOM micelles. In Brazil, hydrophobic structures have been observed in hydromorphic profiles and in soils where SOM is less oxidized due to hydric saturation in the pedoenvironment (Pérez et al., 1998). It is believed that water repellency can be caused by particles being coated by hydrophobic substances. These substances may be derived directly from plant residue decomposition or from specific products of microbial metabolism (DeBano, 2003; Buczko et al., 2005). Possibly, these hydrophobic zones can aid aggregate stabilization by covering organo-mineral complexes and larger structures.

Due to SOM self-association, hydrophobic protection can be a very important aggregation mechanism in C-rich soils. This is the case for humic and histic soil profiles from the high

plain zones of southern Brazil. These studies have been used to evaluate the effect on water retention and environmental filters (Kadlec and Wallace, 2009). Aggregation is one of the most important factors for these soil functions.

These C-rich soils under natural vegetation are an interesting environment to investigate the factors related to SOM that control structural stability since the aggregate stability mechanisms have reached their equilibrium stage. Studies that relate SOM chemical composition to aggregate stability in C-rich environments are rare, yet may contribute to knowledge regarding how SOM acts on the phenomenon of soil aggregation.

The hypothesis of this study was that, under the same environmental conditions, the structural stabilization of aerobic soils is mainly related to the organo-mineral interaction, while in C-rich profiles under hydromorphic conditions, hydrophobic protection is the most relevant mechanism. Thus, the objective of this study was to investigate the aggregate stability mechanisms related to SOM chemical composition in soil profiles with humic and histic horizons in a toposequence under an Araucaria moist forest in southern Brazil.

MATERIALS AND METHODS

Study area and sampling

Soil sampling was performed in a toposequence under an Araucaria moist forest in the sedimentary basin of Curitiba in the "Primeiro Planalto Paranaense" (roughly translated: "first plateau of Parana"), Brazil, located in the environmental protection area of Iraí (EPA-Iraí), a hydrographic microbasin of the Canguiri River.

The soils sampled were derived from sedimentary rocks (Argillite and Arcosian deposits) of the Guabirota Formation. This geologic formation belongs to the Cenozoic Era, with ages ranging from the Miocene to Pleistocene (Salamuni and Stellfeld, 2001; Salamuni et al., 2004). According to Köppen classification system, the climate is classified as Cfb - subtropical humid with moderate winters and mild summers, with annual average rainfall ranging from 1,500 to 1,600 mm and an average temperature of 19.1 °C (Maack, 2012). This region has a sub-dendritic drainage pattern and the slopes range from strongly rolling to rolling in a divergent convex topography. The slopes are attenuated at the top and at the entrance of the floodplain, where there is a flat slope.

Three different soil classes were sampled: i) *Latossolo Bruno Alumínico rúbrico* (Humic Hapludox - OX) - altitude of 951 m, flat to slightly rolling slope (25° 24' 38" S and 49° 7' 34" W); ii) *Gleissolo Melânico Ta Distrófico organossólico* (Fluvaquentic Humaquepts - FH) - altitude of 918 m, slightly rolling slope (25° 24' 39" S and 49° 7' 17" W); iii) *Organossolo Háptico Sáplico típico* (Typic Haplosaprists - TS) - altitude of 913 m, flat slope (25° 24' 40" S and 49° 7' 13" W). In the landscape, the soil profile positions correspond to the top of the slope (non-hydromorphic site); lower third (hydromorphic site - subsurface hydromorphism), and floodplain (hydromorphic site - surface water table for a short period of the year). In each site, three trenches were opened at a distance of approximately 15 m between them and different layers were sampled (0.00-0.05, 0.05-0.10, 0.10-0.15, 0.15-0.20, 0.20-0.30, 0.30-0.40, 0.40-0.60, 0.60-0.80, 0.80-1.00, 1.00-1.20, 1.20-1.40, 1.40-1.60, and 1.60-1.80 m), using triplicate sampling by soil type. In OX, the sampling was performed from the soil surface to the deepest layer (1.80 m - soil rock interface). In the other two soils, sampling was performing from the surface to the depth of the water table (1.0 m for FH and 0.6 m for TS).

During soil sampling, pH was determined in distilled water. In OX, the pH values ranged from 4.0 to 4.9. In FH, the same properties ranged from 4.5 to 4.9 and in TS, from 3.7 to 4.0.

To investigate aggregate stability, undisturbed soil monoliths in replicates of approximately 2 dm³ were collected and transported to the lab in closed containers. Subsequently, the

monoliths were gently disaggregated manually, maintaining field moisture, and sieved (9.51 mm). After air drying, the samples were separated into different aggregate classes using sieves with 4.00, 2.00, 1.00, and 0.25 mm mesh.

Organic carbon and nitrogen content

The C and N contents were determined by dry combustion ("Variol El" elemental analyzer) of the soil bulk samples. The samples had been milled and sieved through a 0.2 mm mesh.

Hydrofluoric acid treatment

Demineralization of the samples was performed according to Gonçalves et al. (2003). In brief, 1 g of soil was weighed and treated with 30 mL of hydrofluoric acid solution (10 %, v/v). The samples were shaken manually for 30 s, followed by horizontal mechanical agitation for 2 h. The material was centrifuged (10 min - relative centrifugal force = 1050) and the supernatant was discarded. This procedure was repeated eight times. At the end, the solid residue containing the concentrated organic matter (SOM_{HF}) was washed three times with distilled water and oven dried at 50 °C.

Fourier Transform Infrared Spectroscopy (FTIR)

The SOM_{HF} samples were analyzed by Fourier transform infrared spectroscopy (FTIR) (Shimadzu 8300) in KBr pellets (1:100), using 32 scans and a resolution of 4 cm⁻¹ in the spectral range of 4000 to 400 cm⁻¹.

The absorption bands were attributed according to Farmer (1974) and Tan (1996). From the FTIR spectra we calculated the aromaticity index (AI) (Chefetz et al., 1996) in which $I_{C=C}$ is the absorption intensity around 1630 cm⁻¹ and I_{C-H} is the absorption intensity around 2920 cm⁻¹, after establishing the baseline between 1800 and 1500 cm⁻¹ and between 3000 and 2800 cm⁻¹.

The relative intensities (RI) of the main absorption bands were calculated, following Gerzabek et al. (2006), by dividing the corrected peak intensity (2950, 1710, 1630, 1540, 1430, 1250, and 1075 cm⁻¹) by the sum of the intensities of all peaks, multiplied by 100 %. The parameters to determine the peak intensities were base1/peak/base2 (cm⁻¹): 3000/2950/2800; 1800/1710/1500; 1800/1630/1500; 1800/1540/1500; 1500/1430/900; 1500/1250/900; and 1500/1075/900.

Aggregate stability and dispersed clay content by ultrasound energy application.

To investigate soil aggregate stability by ultrasonic energy application, approximately 10 g of soil were recomposed from the mass proportions of each aggregate class in the bulk sample. The soil aliquots were moistened by capillarity and allowed to stand for 24 h.

These samples were placed in 100 mL centrifuge glass tubes, to which 80 mL of deionized water was added. The soil mass was converted into volume by particle density, which was determined by the fact that soils with high SOM content tend to show lower particle density values. The method used to determine particle density was described in Claessen (1997). Particle density values observed were higher in OX (mean of 2.63 mm), intermediate in FH (mean of 2.49 mm), and lower in TS (mean of 1.81 mm).

Subsequently, increasing levels of ultrasound energy (0, 50, 100, 200, 400, 600, 800, 1000, 1200, and 1500 J mL⁻¹) were applied to the suspension containing soil and deionized water. The equipment used was a Vibracel VCX 700 previously calibrated according to the method described by Christensen (1992).

The concentration of dispersed clay after energy application was determined by the pipette method (Gee and Bauder, 1986). The data of dispersed clay as a function of the energy level applied were fitted to the equation $y = a(1 - e^{-bx})$, in which "y" is the

dispersed clay concentration and “x” is the energy level. This exponential model shows that the clay dispersion rate is decreasing and that the dispersed clay content tends to the maximum, represented by parameter “a” of the function, in which the amount of ultrasound energy applied (variable “x”) tends to infinity. The energy for total dispersion (E_{max}) of the aggregates was assumed to be required to obtain a dispersed clay content equivalent to 99 % of the parameter “a” value. The energy level for each sample was considered an indicator of aggregate stability.

Water holding capacity in disturbed soil samples

Water holding capacity (WHC) was determined to perform correlation analysis with SOM chemical composition in order to identify changes in the degree of sample hydrophobicity due to hydrophobic groups. These results were used to support the effect of SOM on aggregate stability.

Approximately 10 g of soil was recomposed from the mass proportions of each aggregate class in the bulk samples. These samples were milled, sieved (2 mm), and air dried. The soil was placed in filter paper in a glass funnel in a pre-weighed flask.

Then, about 100 g of distilled water (previously weighed on an analytical balance) was added in small portions to the sample. The funnel was covered with plastic film to avoid water loss by evaporation. After 12 h, the water flask was weighed, and WHC was determined by the quotient for the retained water mass over the dry soil mass.

Statistical analysis

Results were first analyzed by descriptive statistics (mean and standard deviation) to verify natural variability of samples with respect to three replicates. After verifying that, in general, the natural variability of the sample set was low, the means were analyzed by multivariate statistics. To support the multivariate studies, simple linear regressions were also applied.

The multivariate analysis was divided into two parts and the statistical software used were i) MULTIV (beta version 309 for Windows); ii) Statistica 7.0; and iii) BioEstat 5.0. The first step was to verify the numerical distribution of the variables and clusters between sample units in order to investigate the need for sample treatment as separate groups. To do so, principal component analysis (PCA) was applied. The data matrix involving all variables (soil chemical and physical properties and SOM variables) was subjected to vector transformation between variables by a standardized dispersion. Correlation was chosen as a similarity measure.

Subsequently, the dispersion stability of the ordination diagram was verified by a bootstrap test. After confirming data dispersion stability, cluster analysis was applied. Group stability was verified by reapplication of the bootstrap test with 5 % significance ($p < 0.05$). As will be presented later, each of the three soils was considered a distinct group and was treated separately in the second step of multivariate analysis.

The objective of the second step was to investigate the effect of SOM chemical composition on aggregate stability. For that reason, canonical correlation analysis (CCA) was applied. The advantage of this technique was its ability to identify the strongest associations between two variable sets simultaneously, rather than simply calculating simple pairwise correlations (Gittins, 1985; Recio-Vazquez et al., 2014). A smaller number of variables than sample units is required for use of this technique.

As the soil organic C content showed a correlation with aggregate stability (results presented and discussed later), only the RI of the SOM groups (identified by FTIR) were chosen as matrix predictor variables; as predicted variables, the E_{max} values were chosen.

The models examined were constructed from two data matrices that produced two canonical variables: i) a linear combination from the RI of SOM groups; and ii) a linear combination of E_{\max} values. Thus, for each soil, a canonical function (canonical variable) was obtained. This canonical variable describes the aggregate stability as a linear function of the SOM groups.

After this procedure, the RI values of the SOM group for each soil were replaced in the canonical function obtained. These values were correlated with the original E_{\max} values. The objective of this procedure was to evaluate the coefficient of determination (R^2) and the regression significance between the canonical function and aggregate stability.

Finally, the correlation coefficient (r) and the significance of the RI of each organic group with each canonical function were analyzed separately. The objectives of this procedure were to identify the most important chemical groups to obtain the canonical function, as well as to rank the groups according to the R^2 and its significance.

RESULTS AND DISCUSSION

C and N content

The C and N content ranged from 0.9 to 176.2 g kg⁻¹ and from 0.1 to 11.1 g kg⁻¹, respectively (Table 1), and both properties decreased in the order TS > FH > OX. In TS, the C content of all layers was above 80 g kg⁻¹, confirming the occurrence of histic horizons in this profile. In FH, the C content ranged from 67.4 to 90 g kg⁻¹, indicating that this soil is a transition between the mineral soils of the slope and the organic soils of the floodplain.

In OX, the C content ranged from 0.9 to 56 g kg⁻¹, decreasing progressively from the top to the deepest layers (Table 1). In the A horizon (0.00-0.42 m), the properties C content, horizon thickness, color, and base saturation characterize the surface horizon as A humic. The subsurface layers are related to the mineral horizons (Bw and C). As expected, the C and N contents were lower in the subsurface layers than the humic horizon (Table 1). The increase in C contents from the top of the slope to the floodplain confirms the conversion gradient of humic content in histic horizons, with increasing soil water saturation.

The C/N ratio was generally higher in FH (17-24), followed by TS (15-19) and OX (6-18) (Table 1). Changes in the values of the C/N ratio by depth suggest the occurrence of different SOM dynamics in these landscape positions. In OX, the C/N ratio increases up to 0.60 m, reaching 18, and then decreases in depth until C/N = 6 (1.60-1.80 m). In FH, the C/N ratio is, in general, higher than in the other soils, and the C/N values are similar between the different layers. In TS, the C/N ratio tends to increase with depth, indicating relative enrichment of N compounds in the soil surface. This difference is probably related to water regime changes in different landscape locations. The SOM decomposition is more limited in hydromorphic terrains than the more oxidizing conditions at the top of the slope.

SOM chemical composition by FTIR

The SOM_{HF} samples showed the same FTIR spectrum pattern; in figure 1, the FH spectra are shown as an example. The absorption bands observed in the spectra were 3420 cm⁻¹, attributed to the O-H stretching in H-bonds; two bands at 2950 and 2840 cm⁻¹, attributed to the C-H stretching of aliphatic groups; 1710 cm⁻¹, attributed to the C=O stretching of carboxyls; 1630 cm⁻¹, attributed to C=C vibration of aromatic groups; 1540 cm⁻¹, attributed to N-H deformation and to C=N stretching; 1245 cm⁻¹, attributed to C-O stretching and OH deformation of the carboxyl group; and 1075 cm⁻¹, attributed to the C-O bond of primary and secondary alcohols. In SOM studies, this organic function is considered a part of the carbohydrate-like structures (C-O-alkyl).

Table 1. Carbon and N content (mean±standard deviation), FTIR spectral relative intensities, aromatic index, clay content, and water holding capacity of three soils in a toposequence under Araucaria moist forest - Pinhais, PR, Brazil

Depth	C	N	C/N	FTIR relative intensity							AI	Clay	WHC
				RI ₂₉₅₀₋₂₈₄₀	RI ₁₇₁₀	RI ₁₆₃₀	RI ₁₅₄₀	RI ₁₄₃₀₋₁₃₆₀	RI ₁₂₅₀	RI ₁₀₇₅			
m	g kg ⁻¹			%								g kg ⁻¹	g g ⁻¹
Humic Hapludox													
0.00-0.05	54.2±2.2	3.8±2.2	14	12.3	20.0	22.7	6.8	4.5	5.8	27.9	1.8	325±10	0.43±0.01
0.05-0.10	39.2±2.3	2.8±2.3	14	11.1	20.3	27.7	10.4	4.6	6.1	19.8	2.5	303±6	0.42±0.02
0.10-0.15	34.4±1.6	2.4±1.6	15	10.7	21.6	27.6	7.7	8.3	8.3	15.8	2.6	311±6	0.41±0.09
0.15-0.20	32.4±1	2.2±1	15	8.3	22.4	28.7	7.5	10.4	10.0	12.7	3.5	331±4	0.42±0.03
0.20-0.30	29.6±0.7	1.8±0.7	16	8.3	22.2	27.7	6.0	9.4	9.3	17.1	3.3	317±2	0.42±0.01
0.30-0.40	24.6±0.2	1.9±0.2	13	7.7	21.9	26.0	8.2	9.1	11.2	15.9	3.4	329±8	0.41±0.02
0.40-0.60	17.4±0.1	0.9±0.1	18	6.8	22.2	28.7	8.4	11.9	8.9	13.1	4.2	341±7	0.41±0.01
0.60-0.80	8.9±0.6	0.6±0.6	15	6.4	17.5	32.3	11.6	6.1	11.7	14.4	5.0	463±11	0.50±0.01
0.80-1.00	8.2±0.3	0.8±0.3	10	6.0	18.7	35.0	11.5	10.5	6.3	12.0	5.8	491±13	0.48±0.01
1.00-1.20	4.4±0	0.4±0	12	5.2	19.5	40.7	12.4	9.6	5.3	7.3	7.8	497±7	0.50±0.07
1.20-1.40	2.2±0.5	0.2±0.5	11	3.8	25.5	49.8	12.1	3.1	3.2	2.5	13.1	365±2	0.40±0.01
1.40-1.60	1.6±0.1	0.2±0.1	8	3.2	22.9	51.4	11.1	6.7	3.0	1.7	16.1	361±2	0.40±0.01
1.60-1.80	0.9±0.1	0.1±0.1	6	1.2	24.3	55.9	12.2	3.7	1.3	1.4	46.6	403±8	0.41±0.02
Fluvaquentic Humaquepts													
0.00-0.05	70.4±4.3	3.5±0.1	20	4.2	10.3	44.2	2.1	8.7	19.0	11.5	10.5	351±7	1.39±0.04
0.05-0.10	70.4±4.2	3.0±0.2	23	4.8	11.3	46.5	2.3	8.1	16.3	10.7	9.7	385±5	1.18±0.02
0.10-0.15	79.5±2.9	3.7±0.4	21	5.5	13.1	45.8	3.1	4.5	15.3	12.7	8.3	383±9	1.33±0.02
0.15-0.20	70.0±3.7	3.4±0.7	21	4.7	17.4	33.3	2.3	7.8	24.6	9.9	7.1	320±7	1.56±0.01
0.20-0.30	77.2±5.5	3.2±0.2	24	7.9	27.3	31.3	2.1	4.6	14.4	12.4	4.0	439±13	1.15±0.01
0.30-0.40	67.4±8.6	3.2±0.3	21	7.1	19.8	34.5	2.8	4.8	17.8	13.2	4.9	443±9	1.14±0.01
0.40-0.60	67.9±1.4	4.0±0.1	17	6.4	20.7	34.3	2.9	5.0	19.6	11.1	5.4	375±9	1.24±0.01
0.60-0.80	74.3±3.8	4.30.3	17	7.3	15.2	40.6	2.6	5.2	17.0	12.1	5.6	371±4	1.13±0.01
0.80-1.00	89.8±3.9	4.5±0.3	20	10.4	12.5	37.4	3.1	3.6	12.6	20.4	3.6	487±11	0.91±0.04
Typic Haplosaprists													
0.00-0.05	142.6±5.3	9.1±0.4	16	6.5	22.9	24.8	11.1	11.8	15.3	7.6	3.8	175±8	5.59±0.08
0.05-0.10	168.9±3.7	11.1±0.3	15	7.5	25.0	28.5	10.0	9.5	13.5	6.0	3.8	123±7	5.02±0.04
0.10-0.15	169.2±1.9	10.9±0.4	16	7.7	23.1	28.0	11.3	8.2	13.0	8.7	3.6	177±12	4.33±0.14
0.15-0.20	176.2±2.9	10.7±0.2	16	8.3	21.4	23.4	10.7	12.1	16.8	7.3	2.8	159±14	3.87±0.07
0.20-0.30	167.2±0.5	9.5±0	18	7.3	25.5	27.1	13.0	8.1	13.6	5.4	3.7	127±9	4.73±0.04
0.30-0.40	159.3±2	8.6±0.1	19	7.4	26.2	30.4	8.9	6.9	13.8	6.4	4.1	149±9	4.67±0.06
0.40-0.60	100.9±0.4	5.1±0	20	5.9	23.8	26.2	11.7	9.8	15.2	7.4	4.4	187±8	6.25±0.16

C and N: C and N contents determined by dry combustion in a CN elemental analyzer, results presented and discussed in detail in Hanke and Dick (2016); RI: relative intensities of SOM groups determined by Fourier Transform Infrared Spectroscopy (FTIR) after sample demineralization with 10 % HF (v/v); AI: aromatic index calculated by $RI_{1630}/RI_{2950-2840}$; Clay: clay content after ultrasound dispersion and determination by pipette method; WHC: water holding capacity.

In TS, the RI_{1630} ranged from 24.8 to 30.4 %, with similar values throughout the profile (Table 1). In this profile, the AI ranged from 2.8 to 4.4, and the higher values at depth may be the result of older aromatic preservation by hydromorphy.

The RI of carboxylic groups (RI_{1710}) ranged from 10.3 to 27.3 %. In general, these values were higher in OX (21.5±2.2) and TS (24.0±1.7) than in FH (16.4±5.5) (Table 1). The OX profile showed a small tendency to increase RI_{1710} at depth, which is probably related to carboxylated hydrophilic compound percolation (Kalbitz et al., 2000). In TS, hydromorphic conditions may limit the decarboxylation process, which may be considered one of the

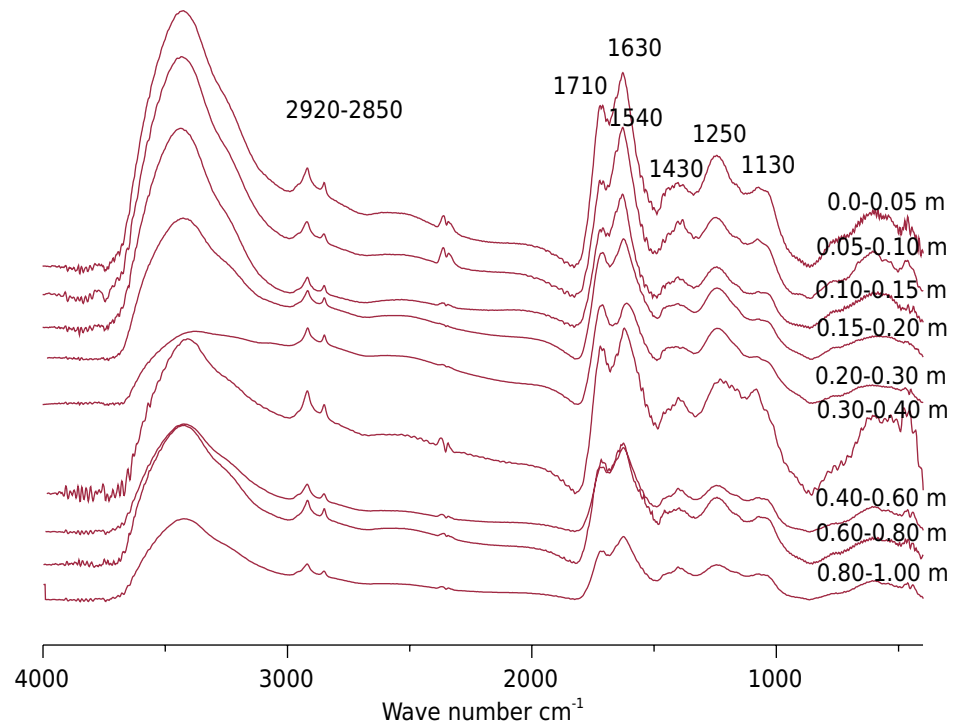


Figure 1. FTIR spectra of soil organic matter after 10 % HF (v/v) treatments of Fluvaqueptic Humaquepts under Araucaria moist forest.

most important processes of SOM oxidative decomposition. The lower redox potential of hydromorphic soils may limit carboxyl breakdown from the structure and, consequently, its conversion to CO_2 . Under these conditions, other biochemical fermentation pathways are used by microorganisms (Nelson and Cox, 2002).

In FH, poor drainage and water table oscillation limit carboxylic compound percolation to deeper soil layers.

In OX, the RI of the N compounds (RI_{1540}) ranged from 6.0 to 12.2 % and increased gradually at depth (Table 1). This increase was associated with a decrease in the C/N ratio, confirming relative enrichment in N structures, which suggests an increasing degree of humification. In TS, the RI_{1540} oscillated around 11 ± 1.3 throughout the profile. The FH profile showed IR_{1540} values much lower (2.6 ± 0.4) than those observed in the other soils, indicating a lower proportion of N compounds. These results are consistent with higher C/N values compared to the other profiles.

The OX soil showed the highest values of RI_{1075} , which decrease from the surface to depth (Table 1). The higher abundance of these groups, with higher biochemical lability in the SOM composition of the surface horizon, is related to the contribution of vegetation biomass. At depth, the proportion of this group decreased, due to its preferential degradation in the aerobic environment. In the FH and TS samples, a positive linear correlation was observed between RI_{1075} and clay content (Figure 2). This result suggests that the C-O groups that are part of carbohydrate-like structures (primary and secondary alcohols), which are more polar than other C-O groups, interact with the polar sites of mineral surfaces. This hypothesis is supported by the higher iron extracted by ammonium oxalate and iron extracted by dithionite-citrate-bicarbonate (Feo/Fed) ratio of FH and TS in comparison to OX (Hanke and Dick, 2017). In these two C-rich soils, the low crystallinity Fe oxide content is higher than in OX and, therefore, they have a higher density of monocoordinated hydroxyls. The reactive sites may interact with C-O-alkyl groups of SOM. The interaction between the carbohydrate-like structures and the clay-mineral surface has been observed by other authors (Schöning et al., 2005; Hanke et al., 2015). This result corroborates the

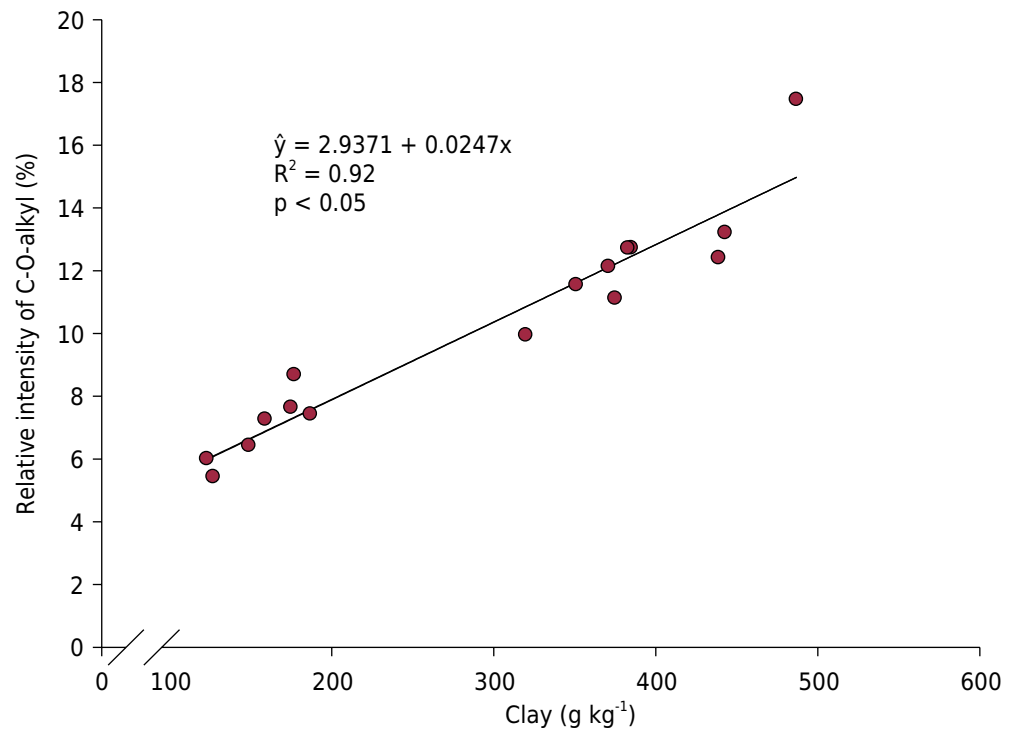


Figure 2. Linear regression between clay content and relative intensity of C-O-alkyl of FH and TS.

existence of a contact zone between SOM and the mineral surface through the action of hydrophilic organic groups (Kleber et al., 2007).

Clay content and aggregate stability

The clay content was similar between OX (303 to 497 g kg⁻¹) and FH (320 to 487 g kg⁻¹), and lower in TS (123 to 187 g kg⁻¹) (Table 1). Sample dispersion, in ultrasonic energy, showed an inflection range of dispersion curves. This range was followed by practically constant values of dispersed clay, indicating the destruction of soil aggregates. Examples of the dispersion curves can be found in figure 3.

The E_{max} values of samples ranged from 33 to 1535 J mL⁻¹ (Figure 4), with lower values in OX and higher in FH and TS (Figure 4). The E_{max} range was lower for soils with higher mineral content (687 and 555 J mL⁻¹ for OX and FH, respectively) and higher for TS (952 J mL⁻¹). However, in OX, the E_{max} decreased progressively at depth (from 720 to 33 J mL⁻¹), with low values in the deepest layer (1.60-1.80 m) and an energy level expressively lower than that observed in the surface layer (0.00-0.05 m). This result highlights the structural fragility in subsurface horizons in comparison to the humic horizon (0.00-0.42 m), in which E_{max} showed a mean value of 529 J mL⁻¹.

In contrast to OX, FH and TS showed E_{max} values ranging randomly between the different layers (Figure 4). In general, these values were high, characterizing high soil structural stability by ultrasound energy.

The SOM effects on aggregate stabilization may be observed in the positive correlation between C content and E_{max} (Figure 5). The slope of the regression line (angular coefficient) decreases in the order FH (24) > TS (15) > OX (13), indicating that C content affects aggregate stability differently in all three soils. In OX, the proportion of C to the clay content is low (C/clay ratio values ranging from 0.002 to 0.17), suggesting the occurrence of a direct interaction between the organic groups and mineral surface (contact zone). In TS, the C/clay ratio was higher, ranging from 0.54 to 1.34, which is due to the low clay content of this profile compared to the other soils. This result suggests C saturation

of the mineral surface, as well as that the SOM effect on aggregation is different from that in OX. In FH, the C/clay ratio values were intermediate, ranging from 0.15 to 0.22, indicating that the SOM effect on aggregation may be a combination of the main processes that occur in OX and TS. In contrast, it may be observed that the aggregate stability of FH and TS is extremely dependent on C content, since the regression intercept values (parameter “a”) are negative. This means that the “ \hat{y} ” value tends to zero when “x = 0”.

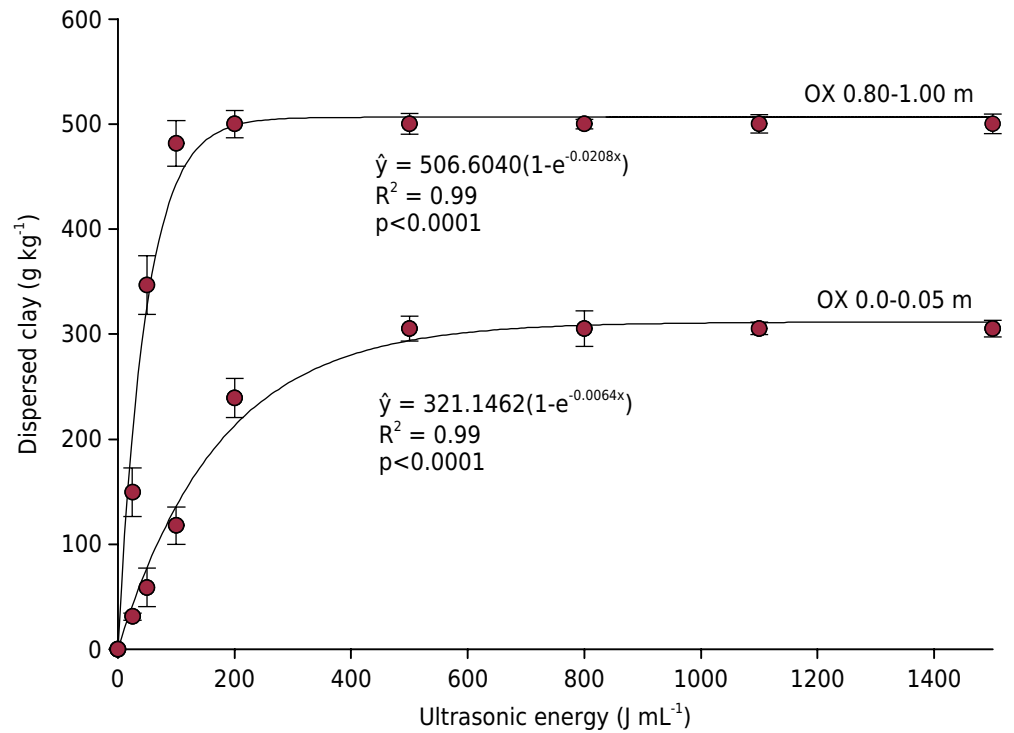


Figure 3. Ultrasound dispersion curves from two different samples of a Humic Hapludox under Araucaria moist forest.

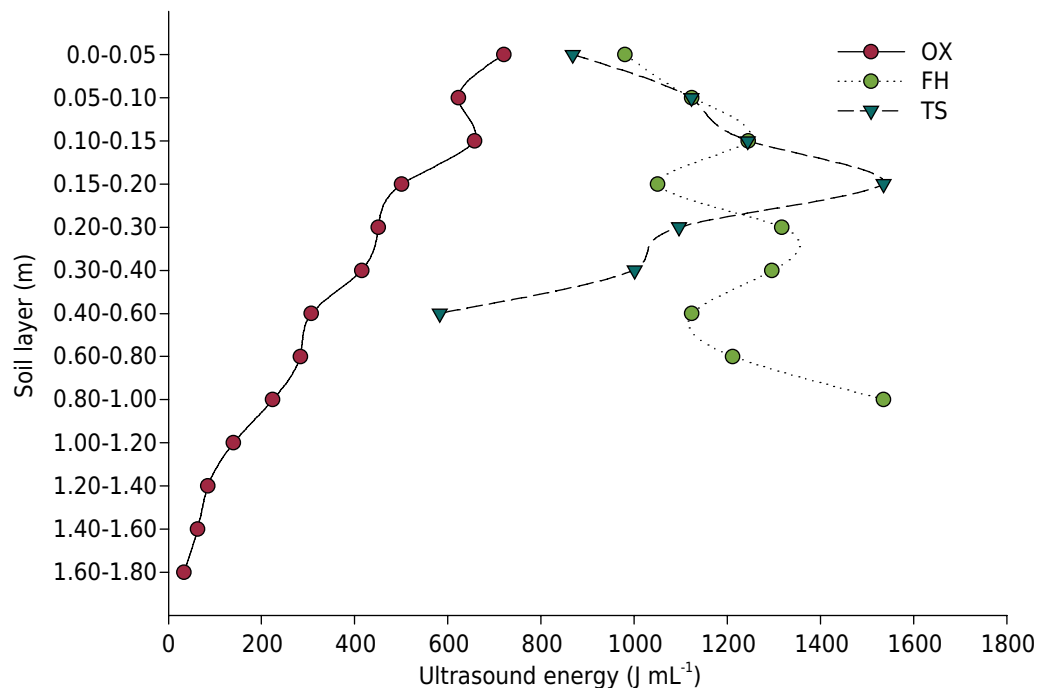


Figure 4. Energy levels for clay dispersion in samples from three different soils along a toposequence in Araucaria moist forest.

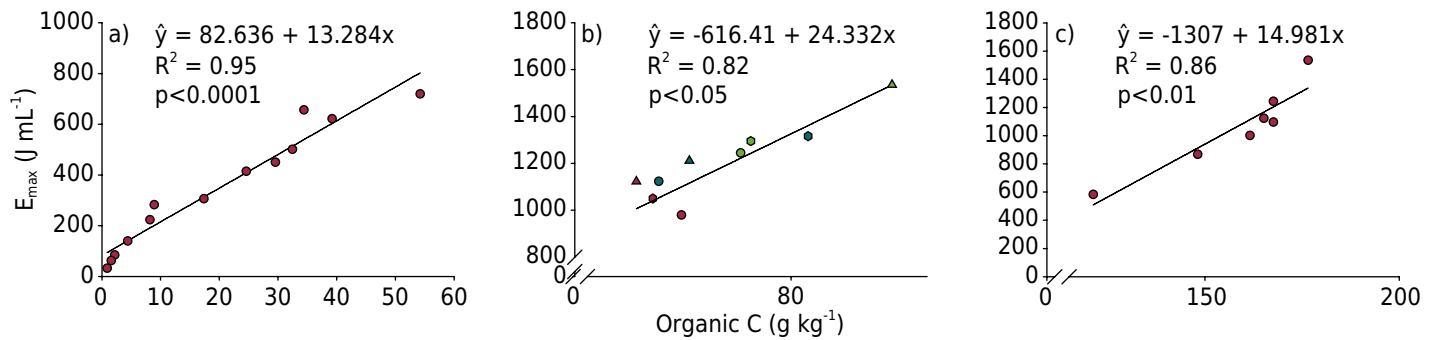


Figure 5. Linear regressions between the organic C content and dispersion energy levels in a) OX, b) FH, and c) TS.

In OX, the intercept value is positive (83), which theoretically represents the action of other soil properties (chemical and mineralogical) on aggregate stability.

In OX, no correlation was observed between clay content and E_{\max} . This suggests that the difference in C content and SOM chemical composition between the layers was more substantial in explaining the differences in structural stability than the textural aspects. In addition, lower aggregate stability was found in the layers with higher clay content in the subsurface.

The absence of a correlation between clay content and aggregate stability was also observed by other authors in studies on weathered soils. This has been attributed to the more pronounced effect of certain clay surfaces on aggregation (Neves et al., 2006; Inda Junior et al., 2007).

In FH, as opposed to OX and TS, the clay content was important in explaining the E_{\max} range between soil layers (positive correlation: $R^2 = 0.88$ and $p < 0.01$). The uniformity of C content between FH layers may have contributed to the texture effect on aggregate stability. In TS, high C content overlaps with the clay effect on aggregation.

Water holding capacity in disturbed soil samples

The WHC of soil samples was higher in TS, with values ranging from 3 to 6 g g⁻¹ (Table 1). In FH, WHC ranged from 0.9 to 1.6 g g⁻¹, and in OX, it was from 0.40 to 0.50 (Table 1). These results confirm the high water storage capacity in histic horizons (TS), as well as in mineral-organic transitional soil (FH).

The values observed in the present study are consistent with those reported for organic horizons by Soil Survey Staff (1992), where the sapric material has a storage capacity of about five times its dry mass. This capacity is lower for pedogenic mineral materials. Therefore, in addition to the potential for C-stock, these soils have high water retention, which is important for water cycle regulation and water distribution along slopes.

Although higher WHC values (TS and FH) were observed in the hydromorphic C-rich soils, no direct correlation was observed between WHC and C content. This suggests that in soils with a high SOM content, C content is not the determining factor, rather SOM chemical composition is. In FH and TS, there is a negative correlation between the RI of the aliphatic groups ($RI_{2950-2840}$) and WHC (Figure 6), indicating that, while these C-rich soils showed higher water storage capacity, the increase of SOM hydrophobicity leads to a decrease in WHC.

The relative aliphatic enrichment of SOM possibly leads to hydrophobic niche formations that repel water entry. In turn, this higher water repellency would contribute to SOM preservation. This occurs by isolation of more labile groups by hydrophobic compounds. This hydrophobic protection has higher biochemical recalcitrance, limiting the action of heterotrophic organisms. Hydrophobic encapsulation also prevents structural collapse

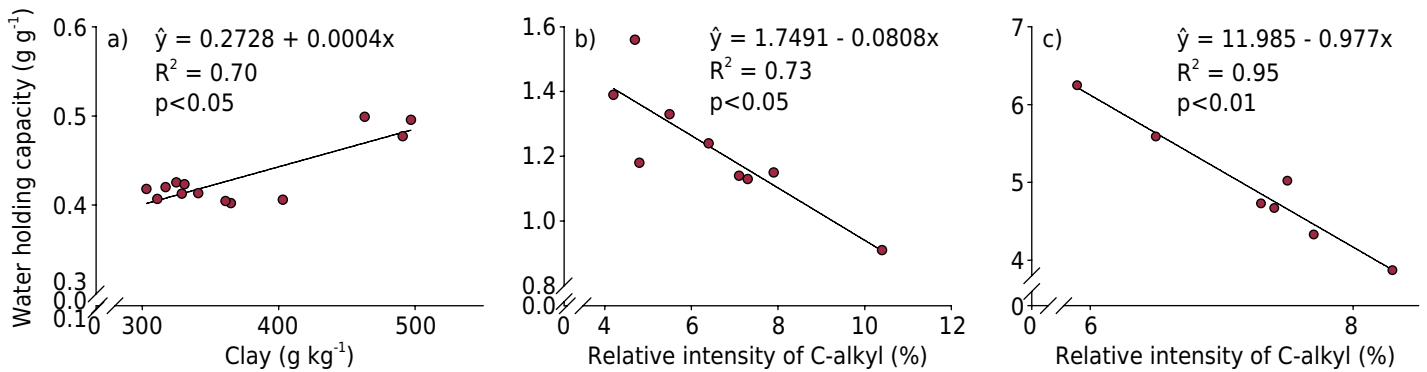


Figure 6. Linear regressions between water holding capacity and a) clay content in OX, b) relative intensity of C-alkyl in FH, c) relative intensity of C-alkyl in TS.

by the instantaneous exit of internal air from the aggregate in the presence of water. For that reason, this hydrophobic mechanism could contribute to aggregate stability and lead to SOM preservation inside these structures (Ellerbrock et al., 2005). Thus, there is a synergism between aggregate protection by hydrophobic structures and SOM preservation by physical occlusion of organic material.

In OX, this correlation was not observed, possibly due to the greater importance of surface adsorption mechanisms to water retention in the clay fraction (Figure 6). In this case, contrary to that observed in FH and TS, the contribution of the clay fraction to WHC overlaps with the contribution of SOM chemical composition. In FH and TS, although the increase in hydrophobicity may contribute to SOM preservation through biochemical recalcitrance, as well as an increase in aggregate stability, this characteristic may reduce the WHC (Ellerbrock et al., 2005).

Our results showed that for low SOM content, the WHC is governed by clay content. Although no direct relationship was observed, the increase in SOM content leads to an increase in WHC, which decreased in the order TS > FH > OX. However, for the C-rich environments, the WHC range seems to be conditioned by the SOM chemical composition. That is, the relative enrichment of aliphatic groups leads to the formation of hydrophobic niches that repel water entry and decrease WHC. The high WHC of hydromorphic soils, associated with higher C contents, emphasizes its importance in the maintenance of very specific environmental conditions. These environmental conditions act as important support for the local fauna and flora that need to be preserved.

SOM and aggregate stability - principal component analysis and canonical correlation

In order to verify the sample unit distribution and group formation in relation to SOM composition and aggregate stability, principal component analysis (PCA) was performed in association with cluster analysis. The SOM variables (C and N content, C/N ratio, and the RI of SOM groups) and E_{max} values were used for this purpose. By the bootstrap resampling test, only three main components (axes) were considered valid ($p < 0.05$) and approximately 91 % of total variance could be explained by these components. Of this proportion, about 79 % of the variance is described by components 1 and 2, that is, 72 % of total variance (Figure 7).

Cluster analysis identified the group formation from the sample units for each soil. This result corroborates the sample dispersion pattern in the ordination diagram (Figure 7). However, a greater similarity was observed between the sample of the OX surface horizon and FH samples, which is mainly due to higher C and N content, higher C/N ratio, higher RI of aliphatic and nitrogen groups, and higher aggregate stability. In turn, the OX samples formed an isolated group, strongly described by the variables E_{max} , C-alkyl, C and N, carboxyl, and C-O-alkyl. The bootstrap resampling test performed in cluster

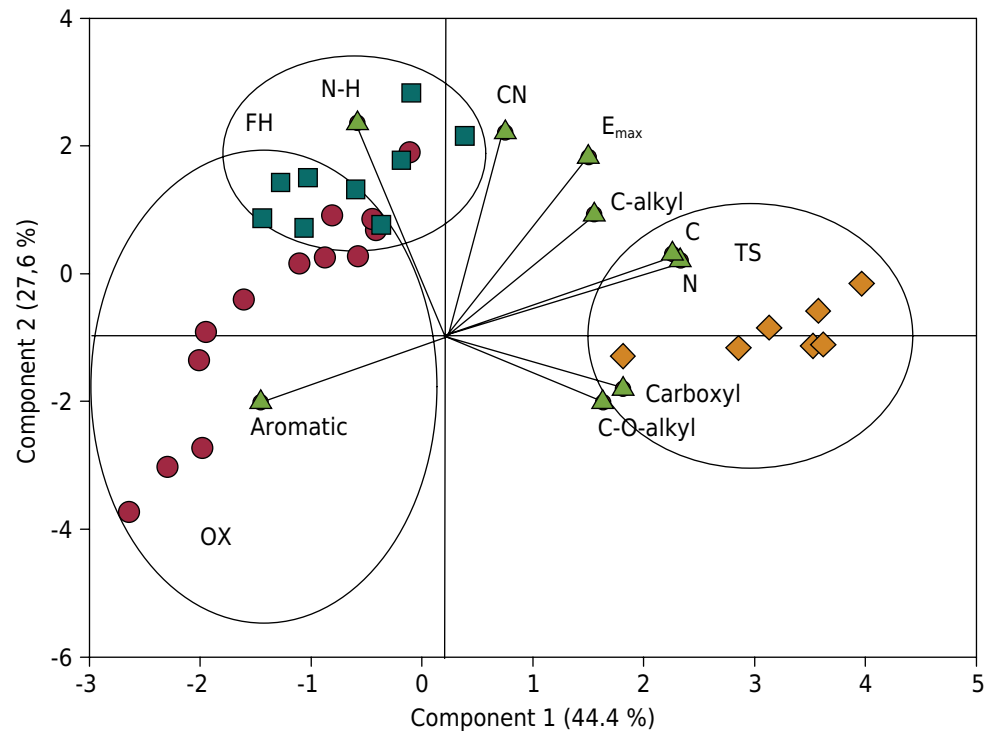


Figure 7. Dispersion diagram by principal component analysis (PCA) showing the soil classes as distinct groups.

analysis confirmed the stability of these three groups ($p < 0.05$). Thus, each soil class of a toposequence characterizes a specific environment and, for the purpose of this study, was analyzed separately.

Considering that the C content showed a positive correlation with the aggregate stability parameter (Figure 5) and in the interest of studying only the relationship between the SOM chemical composition with this property, we used canonical correlation analysis (CCA). In this analysis, the RI of different functional SOM groups were considered as an independent variable set, and the E_{max} as a dependent variable.

The description of canonical functions, their significance, and their correlation with aggregate stability for each soil and the statistical parameters of each regression model are presented in figure 8. The weight of each independent variable in the canonical function is presented in table 2.

The canonical predictor variables (canonical functions), composed of the RI of the SOM groups, were significant ($p < 0.05$) for the three soils analyzed. The correlation between these variables and E_{max} was likewise high. However, only some organic groups were considered valid considering the correlation coefficients between each group and the canonical function ($r > 0.50$). Based on the coefficient of determination (R^2), the significant organic groups were ranked for each canonical function (Table 2).

In OX, the two most important organic groups were C-O-alkyl and C-alkyl; it should be noted that the effect of carbohydrate-like structures was higher than aliphatic chains for soil aggregation (Table 2). A similar response was observed in FH, in which the same groups were considered relevant for aggregate stability. These results suggest that in mineral soils, the importance of more labile and polar structures, such as C-O-alkyl groups, is more pronounced due to the higher clay content. The reactive hydroxyls on the clay-mineral surface may interact with SOM polar groups forming organo-mineral complexes. In a second mechanism, the C-alkyl structures would self-associate, forming a second zone of hydrophobic interactions (Kleber et al., 2007). This hydrophobic zone may contribute to the increase of structural stability by the physical protection of aggregates.

In FH, both C-O-alkyl and C-alkyl groups were important for aggregate stability. This was probably due to the fact that FH is a transitional condition between organic and mineral soils. However, the higher R^2 of aliphatic structures (Table 2) suggests there is a more significant contribution of a hydrophobic protection mechanism than in OX. Probably, the

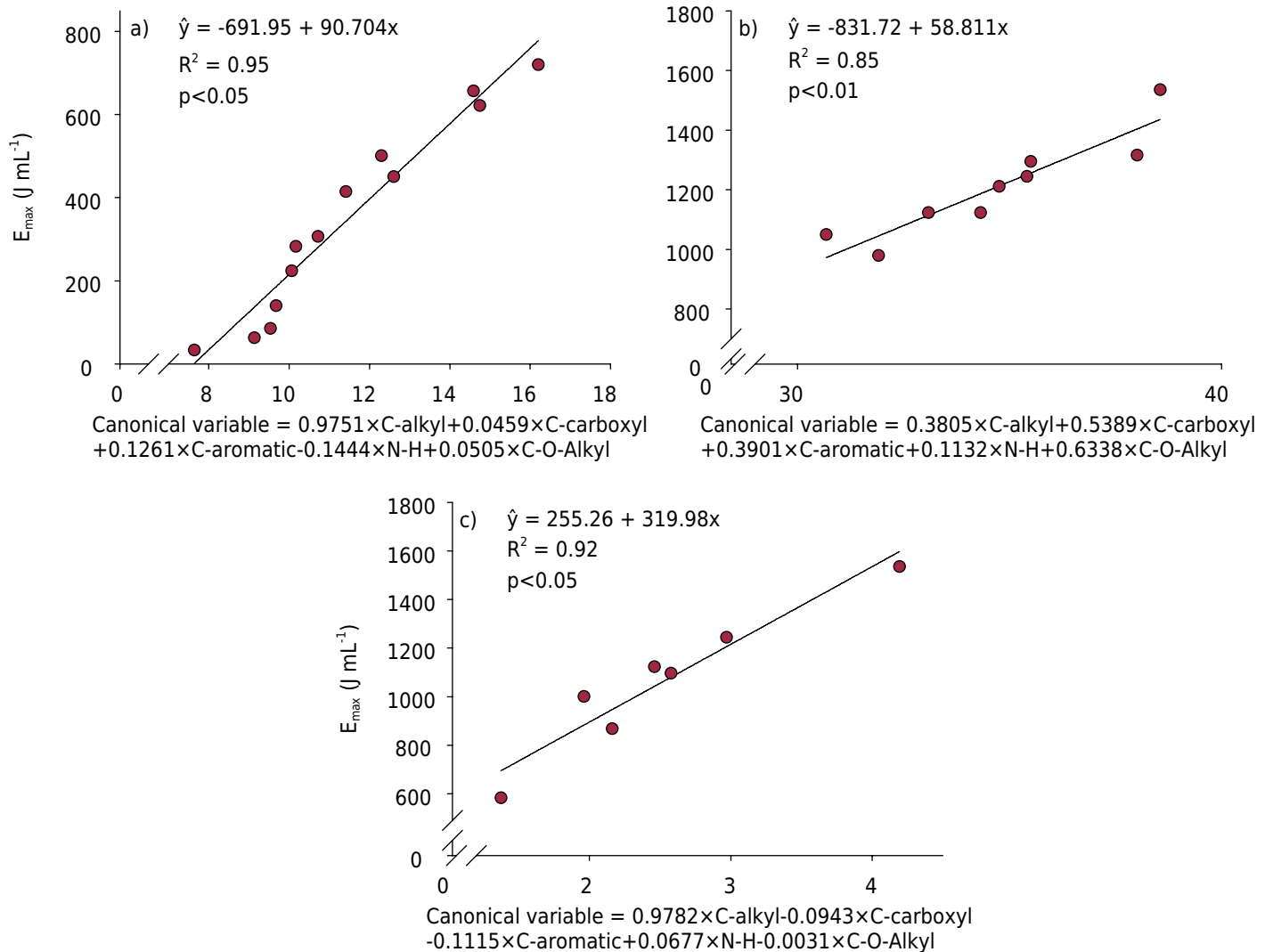


Figure 8. Linear regressions between the canonical variable and the ultrasound energy levels in a) OX, b) FH, and c) TS.

Table 2. Canonical variables produced by SOM chemical groups, canonical coefficient of determination, and significance and ranking of organic groups for each canonical variable

Soil	X canonical variable	Canonical R^2	p				
OX	$X_i = 0.9751 \times \text{C-alkyl} + 0.0459 \times \text{C-carboxyl} + 0.1261 \times \text{C-aromatic} - 0.1444 \times \text{N-H} + 0.0505 \times \text{C-O-alkyl}$	0.9866	<0.0001				
FH	$X_i = 0.3805 \times \text{C-alkyl} + 0.5383 \times \text{C-carboxyl} + 0.3901 \times \text{C-aromatic} + 0.1132 \times \text{N-H} + 0.6338 \times \text{C-O-alkyl}$	0.9701	0.0082				
TS	$X_i = 0.9782 \times \text{C-alkyl} - 0.0943 \times \text{C-carboxyl} - 0.1115 \times \text{C-aromatic} + 0.0677 \times \text{N-H} - 0.0031 \times \text{C-O-alkyl}$	0.9989	0.0007				
Correlation between the SOM and canonical variables							
	C-alkyl	C-carboxyl	C-aromatic	N-H	C-O-alkyl	Ranking of significant variables	
						1 ^o	2 ^o
OX	0.992*	-0.317	-0.3902	-0.3815	0.9235*	C-O-alkyl ($R^2=0.98$)	C-alkyl ($R^2=0.85$)
FH	0.9583*	0.195	-0.2708	0.4909	0.8981*	C-alkyl ($R^2=0.92$)	C-O-alkyl ($R^2=0.81$)
TS	0.9737*	-0.3691	-0.1957	-0.1323	0.0327	C-alkyl ($R^2=0.95$)	-

*: significance ($p=0.05$).

higher C content and lower clay content compared to OX favor mineral surface saturation by C, as well as SOM self-association.

In TS, only the C-alkyl structures were significant for determining the canonical function. In this soil, although a significant correlation was observed between the clay content and RI of C-O-alkyl groups (Table 2), the carbohydrate-like structures were not relevant in explaining aggregate stability. This result is due to the high C content and the lower density of mineral sites (mean of clay content = 156 g kg^{-1}) for interaction with polar SOM groups, favoring mineral surface saturation by SOM and aliphatic association. Thus, the protection conferred by the hydrophobic structures (C-alkyl) was the predominant mechanism in soil structural stability.

Our results suggest that there is a transition between structural stability mechanisms according to toposequence position: i) in the non-hydromorphic positions, where soils are weathered and have lower C content, the organo-mineral interaction is more expressive; and ii) in hydromorphic positions (lower third and floodplain), the hydrophobic physical protection is the most important mechanism. However, this does not mean that in FH and TS strong interactions between SOM groups and lower crystallinity Fe oxides cannot occur. Ferridrite and Lepidocrocite are typically found in C-rich environments, as well as in flooded soils. In fact, the Feo/Fed ratio in FH and TS ranged from 0.46 to 1.0. The same ratio in OX showed very low values (Hanke and Dick, 2017), confirming the higher proportion of lower crystallinity oxides in C-rich soils. However, this mechanistic contribution may be less important than the protection conferred by the aliphatic zone, which was confirmed by the CCA.

The existence of a transition between the aggregate stability mechanisms in the toposequence, related to the polar and apolar SOM compounds, can be supported by the correlations between the WHC and the E_{max} in each profile. Whereas in OX there was no significant correlation between these two attributes ($R^2 = 0.02$), in FH and OX, this correlation was significant ($p < 0.01$).

One of the main mechanisms that break the aggregates is water entry, which causes instantaneous air expulsion, collapsing the structure (Sullivan, 1990). In addition, separation between the components by the increase in the water layer is also responsible for the rupture. This is due to cohesive force reduction and particle adhesion, causing the component dispersion. Therefore, the existence of stable organo-mineral complexes and the protection conferred by hydrophobic groups are important for aggregate stabilization.

CONCLUSIONS

Both C-alkyl and C-O-alkyl groups are important for aggregate stability as determined by ultrasound energy.

In the more weathered soil (OX), organo-mineral interactions between the C-O-alkyl groups and the clay surface seem to be the most important aggregation mechanism. In C-rich soils of lower toposequence positions (FH and TS), the predominant stability mechanism seems to be the physical protection conferred by hydrophobic structure self-association involving C-alkyl groups.

Higher ultrasonic energy values for clay dispersion are observed in the C-rich soils (TS and FH), indicating that organic compounds play an important role in structural stability. Considering that changes in soil use and management may be reflected in changes in SOM chemical composition, a decrease in the structural stability and C-stock capacity of these soils is expected. Therefore, future studies comparing natural and anthropic systems under the same environmental conditions could contribute to understanding the influence of human activities on aggregation mechanisms related to SOM.

REFERENCES

- Barthès BG, Kouakoua E, Larré-Larrouy MC, Razafimbelo TM, De Luca EF, Azontonde A, Neves CSVJ, De Freitas PL, Feller CL. Texture and sesquioxide effects on water-stable aggregates and organic matter in some tropical soils. *Geoderma*. 2008;143:14-25. <https://doi.org/10.1016/j.geoderma.2007.10.003>
- Berhe AA, Kleber M. Erosion, deposition, and the persistence of soil organic matter: mechanistic considerations and problems with terminology. *Earth Surf Proc Land*. 2013;38:908-12. <https://doi.org/10.1002/esp.3408>
- Buczko U, Bens O, Hüttl RF. Variability of soil water repellency in Sandy Forest soils with different stand structure under Scots pine (*Pinus sylvestris*) and beech (*Fagus sylvatica*). *Geoderma*. 2005;126:317-36. <https://doi.org/10.1016/j.geoderma.2004.10.003>
- Chaney K, Swift RS. The influence of organic matter on aggregate stability in some British soils. *J Soil Sci*. 1984;35:223-30. <https://doi.org/10.1111/j.1365-2389.1984.tb00278.x>
- Chaplot V, Cooper M. Soil aggregate stability to predict organic carbon outputs from soils. *Geoderma*. 2015;243-244:205-13. <https://doi.org/10.1016/j.geoderma.2014.12.013>
- Chefetz B, Hatcher P, Hadar Y, Chen Y. Chemical and biological characterization of organic matter during composting of municipal solid waste. *J Environ Qual*. 1996;25:776-85. <https://doi.org/10.2134/jeq1996.00472425002500040018x>
- Chorover J, Amistadi MK. Reaction of forest floor organic matter at goethite, birnessite and smectite surfaces. *Geochim Cosmochim Acta*. 2001;65:95-109. [https://doi.org/10.1016/S0016-7037\(00\)00511-1](https://doi.org/10.1016/S0016-7037(00)00511-1)
- Christensen BT. Physical fractionation of soil and organic matter in primary particle size and density separates. *Adv Soil Sci*. 1992;20:1-90.
- Claessen MEC, organizador. Manual de métodos de análise de solo. 2a ed. Rio de Janeiro: Centro Nacional de Pesquisa de Solos; 1997.
- DeBano LF. The role of fire and soil heating on water repellency. In: Ritsema CJ, Dekker LW, editors. *Soil water repellency: occurrence, consequences, and amelioration*. Amsterdam: Elsevier Science; 2003. p.193-202.
- Dick DP, Novotny EH, Dieckow J, Bayer C. Química da matéria orgânica do solo. In: Melo VF, Alleoni LRF, editores. *Química e mineralogia do solo*. Viçosa, MG: Sociedade Brasileira de Ciência do Solo; 2009. p.1-67.
- Ellerbrock RH, Gerke HH, Bachmann J, Goebel MO. Composition of organic matter fractions for explaining wettability of three forest soils. *Soil Sci Soc Am J*. 2005;69:57-66. <https://doi.org/10.2136/sssaj2005.0057>
- Farmer VC. *The infrared spectra of minerals*. Surrey: Mineralogical Society; 1974.
- Gajic B, Dugalic G, Djurovic N. Comparison of soil organic matter content, aggregate composition and water stability of Gleyic Fluvisol from adjacent forest area and cultivated areas. *Agron Res*. 2006;4:499-508.
- Gee GW, Bauder JW. Particle-size analysis. In: Klute A, editor. *Methods of soil analysis. Physical and mineralogical methods*. 2nd ed. Madison: American Society of Agronomy; 1986. Pt 1. p.383-411.
- Gerzabek MH, Antil RS, Kögel-Knabner I, Knicker H, Kirchmann H, Haberhauer G. How are soil use and management reflected by soil organic matter characteristics: a spectroscopic approach. *Eur J Soil Sci*. 2006;57:485-94. <https://doi.org/10.1111/j.1365-2389.2006.00794.x>
- Gittins R. *Canonical analysis: A review with applications in ecology*. Berlin: Springer-Verlag; 1985.
- Goldberg S, Suarez DL, Glaubig RA. Factors affecting clay dispersion and aggregate stability of arid zone soils. *Soil Sci*. 1988;146:317-25. <https://doi.org/10.1097/00010694-198811000-00004>
- Gonçalves CN, Dalmolin RSD, Dick DP, Knicker H, Klamt E, Kögel-Knabner I. The effect of 10% HF treatment in the resolution of CPMAS ¹³C NMR spectra and on the quality of organic matter in Ferralsols. *Geoderma*. 2003;116:373-92. [https://doi.org/10.1016/S0016-7061\(03\)00119-8](https://doi.org/10.1016/S0016-7061(03)00119-8)
- Hanke D, Dick DP. Organic matter stocks and the interactions of humic substances with araucaria moist forest soil metals with humic and histic horizons. *Rev Bras Cienc Solo*. 2017 (accepted).

- Hanke D, Melo VF, Dieckow J, Dick DP, Bognola IA. Influência da matéria orgânica no diâmetro médio de minerais da fração argila de solos desenvolvidos de basalto no sul do Brasil. *Rev Bras Cienc Solo*. 2015;39:1611-22. <https://doi.org/10.1590/01000683rbcs20140655>
- Igwe CA, Zarei M, Stahr K. Colloidal stability in some tropical soils of southeastern Nigeria as affected by iron and aluminium oxides. *Catena*. 2009;77:232-7. <https://doi.org/10.1016/j.catena.2009.01.003>
- Inda Junior AV, Bayer C, Conceição PC, Boeni M, Salton JC, Tonin AT. Variáveis relacionadas à estabilidade de complexos organo-minerais em solos tropicais e subtropicais brasileiros. *Cienc Rural*. 2007;37:1301-7. <https://doi.org/10.1590/S0103-84782007000500013>
- Kadlec RH, Wallace SD. *Treatment wetlands*. 2nd ed. Boca Raton: CRC Press; 2009.
- Kalbitz K, Solinger S, Park JH, Michalzik B, Matzner E. Controls on the dynamics of dissolved organic matter in soils: a review. *Soil Sci*. 2000;165:277-304. <https://doi.org/10.1097/00010694-200004000-00001>
- Kleber M, Sollins P, Sutton R. A conceptual model of organo-mineral interactions in soils: self-assembly of organic molecular fragments into zonal structures on mineral surfaces. *Biogeochemistry*. 2007;85:9-24. <https://doi.org/10.1007/s10533-007-9103-5>
- Kodešová R, Kočárek M, Kodeš V, Šimůnek J, Kozák J. Impact of soil micromorphological features on water flow and herbicide transport in soil. *Vadose Zone J*. 2008;7:798-809. <https://doi.org/10.2136/vzj2007.0079>
- Kodešová R, Rohošková M, Žigová A. Comparison of aggregate stability within six soil profiles under conventional tillage using various laboratory tests. *Biologia*. 2009;64:550-4. <https://doi.org/10.2478/s11756-009-0095-6>
- Krull ES, Skjemstad JO, Graetz D, Grice K, Dunning W, Cook G, Parr JF. ¹³C-depleted charcoal from C4 grasses and the role of occluded carbon in phytoliths. *Org Geochem*. 2003;34:1337-52. [https://doi.org/10.1016/S0146-6380\(03\)00100-1](https://doi.org/10.1016/S0146-6380(03)00100-1)
- Li H, Han X, Wang F, Qiao Y, Xing B. Impact of soil management on organic carbon content and aggregate stability. *Commun Soil Sci Plant Anal*. 2007;38:1673-90. <https://doi.org/10.1080/00103620701435456>
- Maack R. *Geografia física do Estado do Paraná*. 4a ed. Rio de Janeiro: UEPG; 2012.
- Mikutta R, Zang U, Chorover J, Haumaier L, Kalbitz K. Stabilization of extracellular polymeric substances (*Bacillus subtilis*) by adsorption to and coprecipitation with Al forms. *Geochim Cosmochim Acta*. 2011;75:3135-54. <https://doi.org/10.1016/j.gca.2011.03.006>
- Miltner A, Zech W. Carbohydrate decomposition in beech litter as influenced by aluminium, iron and manganese oxides. *Soil Biol Biochem*. 1998;30:1-7. [https://doi.org/10.1016/S0038-0717\(97\)00092-8](https://doi.org/10.1016/S0038-0717(97)00092-8)
- Nelson DL, Cox MM. *Lehninger - Princípios de Bioquímica*. 3a ed. São Paulo: Sarvier; 2002.
- Neves CSVJ, Feller C, Kouakoua E. Efeito do manejo do solo e da matéria orgânica solúvel em água quente na estabilidade de agregados de um Latossolo argiloso. *Cienc Rural*. 2006;36:1410-5. <https://doi.org/10.1590/S0103-84782006000500010>
- Novara A, La Mantia T, Barbera V, Gristina L. Paired-site approach for studying soil organic carbon dynamics in a Mediterranean semiarid environment. *Catena*. 2012;89:1-7. <https://doi.org/10.1016/j.catena.2011.09.008>
- Pérez DV, Simão SM, Salatino A. Identificação e caracterização da repelência à água em alguns solos brasileiros. *Rev Bras Cienc Solo*. 1998;22:197-207. <https://doi.org/10.1590/S0100-06831998000200004>
- Pinheiro-Dick D, Schwertmann U. Microagregates from Oxisols and Inceptisols: Dispersion through selective dissolutions and physicochemical treatments. *Geoderma*. 1996;74:49-63. [https://doi.org/10.1016/S0016-7061\(96\)00047-X](https://doi.org/10.1016/S0016-7061(96)00047-X)
- Recio-Vazquez L, Almendros G, Knicker H, Carral P, Álvarez AM. Multivariate statistical assessment of functional relationships between soil physical descriptors and structural features of soil organic matter in Mediterranean ecosystems. *Geoderma*. 2014;230-231:95-107. <https://doi.org/10.1016/j.geoderma.2014.04.002>

- Salamuni E, Stellfeld MC. Banco de dados geológicos geo-referenciados da Bacia Sedimentar de Curitiba (PR) como base de Sistema de Informação Geográfica (SIG). *Bol Paranaense Geocienc.* 2001;49:21-31.
- Salamuni E, Ebert HD, Hasui Y. Morfotectônica da bacia sedimentar de Curitiba. *Rev Bras Geocienc.* 2004;34:469-78.
- Scheer MB, Curcio GR, Roderjan CV. Funcionalidades ambientais de solos altomontanos na Serra da Igreja, Paraná. *Rev Bras Cienc Solo.* 2011; 35:1113-26. <https://doi.org/10.1590/S0100-06832011000400005>
- Schmidt MWI, Torn MS, Abiven S, Dittmar T, Guggenberger G, Janssens IA, Kleber M, Kögel-Knabner I, Lehmann J, Manning DA, Nannipieri P, Rasse DP, Weiner S, Trumbore SE. Persistence of soil organic matter as an ecosystem property. *Nature.* 2011;478:49-56. <https://doi.org/10.1038/nature10386>
- Schöning I, Knicker H, Kögel-Knabner I. Intimate association between O/N-alkyl carbon and iron oxides in clay fractions of forest soils. *Org Geochem.* 2005;36:1378-90. <https://doi.org/10.1016/j.orggeochem.2005.06.005>
- Seta AK, Karathanasis AD. Water dispersible colloids and factors influencing their dispersibility from soil aggregates. *Geoderma.* 1996;74:255-66. [https://doi.org/10.1016/S0016-7061\(96\)00066-3](https://doi.org/10.1016/S0016-7061(96)00066-3)
- Six J, Feller C, Denef K, Ogle SM, Sa JCM, Albrecht A. Soil organic matter, biota and aggregation in temperate and tropical soils: effects of no-tillage. *Agronomie.* 2002;22:755-75. <https://doi.org/10.1051/agro:2002043>
- Six J, Bossuyt H, Degryse S, Denef K. A history of research on the link between (micro) aggregates, soil biota, and soil organic matter dynamics. *Soil Till Res.* 2004;79:7-31. <https://doi.org/10.1016/j.still.2004.03.008>
- Soil Survey Staff. *Keys to soil taxonomy.* 5th ed. Virginia: Pocahontas Press; 1992.
- Stumm W. *Chemistry of the solid-water interface.* New York: John Wiley; 1992.
- Sullivan LA. Soil organic matter, air encapsulation and water stable aggregation. *J Soil Sci.* 1990;41:529-34. <https://doi.org/10.1111/j.1365-2389.1990.tb00084.x>
- Tan KH. Infrared spectroscopy. In: Tan HK, editor. *Soil sampling, preparation and analysis.* New York: Marcel Dekker; 1996. p.278-98.
- Wershaw RL, Llaguno EC, Leenheer JA, Sperline RP, Song Y. Mechanism of formation of humus coatings on mineral surfaces 2. Attenuated total reflectance spectra of hydrophobic and hydrophilic fractions of organic acids from compost leachate on alumina. *Colloids Surf A: Physicochem Eng Aspects.* 1996;108:199-211. [https://doi.org/10.1016/0927-7757\(95\)03401-3](https://doi.org/10.1016/0927-7757(95)03401-3)
- Wiseman CLS, Püttmann W. Soil organic carbon and its sorptive preservation in central Germany. *Eur J Soil Sci.* 2005;56:65-76. <https://doi.org/10.1111/j.1351-0754.2004.00655.x>
- Wiseman CLS, Püttmann W. Interactions between mineral phases in the preservation of soil organic matter. *Geoderma.* 2006;134:109-18. <https://doi.org/10.1016/j.geoderma.2005.09.001>